

Synthesis and Reactivity of  $[\text{Fe}_3(\text{CO})_9\text{Te}]^{2-}$ 

Lisa C. Roof, Donna M. Smith, Gregory W. Drake, William T. Pennington, and Joseph W. Kolis\*

Department of Chemistry, Clemson University, Clemson, South Carolina 29634

Received October 8, 1993<sup>⊗</sup>

The reaction of  $\text{Te}^{2-}$  with three equiv of  $\text{Fe}(\text{CO})_5$  leads to formation of  $[\text{Fe}_3(\text{CO})_9(\mu_3\text{-Te})]^{2-}$  (I) in nearly quantitative yield. The structure consists of a three-iron triangle capped by a telluride. Since the compound could be prepared so easily, its reactivity was probed toward a variety of electrophiles, particularly in regard to the reactivity of the lone pair of electrons presumed to reside on the apical telluride. One or two equivalents of acids results in addition of protons across Fe–Fe bonds, while  $\text{NO}^+$  leads to displacement of one CO and formation of  $[\text{Fe}_3(\text{CO})_8(\text{NO})(\mu_3\text{-Te})]^-$ . Softer electrophiles such as  $\text{PPh}_3\text{Au}^+$  and  $\text{PhHg}^+$  also simply add across an Fe–Fe edge of the cluster to form a salt of  $[\text{Fe}_3(\text{CO})_9(\mu_3\text{-Te})(\mu\text{-AuPPh}_3)]^-$  (II). Thus, none of the electrophiles investigated appear to react with the apical telluride. Molecule I also reacts with oxidants as well. Air oxidation of an initial reaction mixture of  $\text{Fe}(\text{CO})_5$  and  $\text{Te}^{2-}$  results in formation of low yields of a salt of  $[(\text{Fe}(\text{CO})_4)_4\text{Te}]^{2-}$  (III). This compound appears to be a byproduct, rather than a result, of a reaction of I with  $\text{O}_2$ . One equivalent of  $\text{I}_2$  leads to formation of a salt of  $[\text{Fe}_3\text{Te}_2(\text{CO})_9\text{I}]^-$  (IV), which is isostructural with the well-known  $\text{Fe}_3\text{Te}_2(\text{CO})_{10}$ . Crystal structure data: for  $[(\text{C}_6\text{H}_5)_4\text{P}]_2[\text{Fe}_3(\text{CO})_9(\mu_3\text{-Te})]$  (I), monoclinic,  $P2_1/n$ ,  $a = 11.034(3)$  Å,  $b = 22.214(8)$  Å,  $c = 21.980(8)$  Å,  $\beta = 97.72(3)^\circ$ ,  $V = 5339(3)$  Å<sup>3</sup>,  $Z = 4$ ,  $R = 0.0819$ ,  $R_w = 0.097$ ; for  $[(\text{C}_6\text{H}_5)_4\text{P}][\text{Fe}_3(\text{CO})_9(\mu_3\text{-Te})(\mu\text{-AuPPh}_3)]$  (II), monoclinic,  $P2_1/c$ ,  $a = 16.970(5)$  Å,  $b = 13.996(4)$  Å,  $c = 21.108(8)$  Å,  $\beta = 95.25(3)^\circ$ ,  $V = 4992(3)$  Å<sup>3</sup>,  $Z = 4$ ,  $R = 0.0507$ ,  $R_w = 0.0579$ ; for  $[(\text{C}_6\text{H}_5)_4\text{P}][(\text{Fe}(\text{CO})_4)_4\text{Te}]$  (III), monoclinic,  $C2/c$ ,  $a = 14.264(4)$  Å,  $b = 19.719(5)$  Å,  $c = 22.937(10)$  Å,  $\beta = 90.55(3)^\circ$ ,  $V = 6451(3)$  Å<sup>3</sup>,  $Z = 4$ ,  $R = 0.0454$ ,  $R_w = 0.0524$ ; for  $[(\text{C}_6\text{H}_5)_4\text{P}][\text{Fe}_3\text{Te}_2(\text{CO})_9\text{I}]$  (IV), triclinic,  $P\bar{1}$ ,  $a = 9.614(1)$  Å,  $b = 14.511(2)$  Å,  $c = 14.668(2)$  Å,  $\alpha = 74.47(1)^\circ$ ,  $\beta = 71.14(1)^\circ$ ,  $\gamma = 83.22(1)^\circ$ ,  $V = 1852.7(5)$  Å<sup>3</sup>,  $Z = 2$ ,  $R = 0.0398$ ,  $R_w = 0.0542$ .

## Introduction

The chemistry of the soluble metal chalcogenides has received widespread attention recently,<sup>1</sup> due in part to their ability to form new metal–main group hybrid clusters, as well as new solid phases.<sup>2</sup> In particular, it has been found that soluble Zintl phases are excellent reagents for the preparation of new transition metal–main group clusters.<sup>1a,c,d</sup> We have been investigating the coordination chemistry of soluble polychalcogenides with simple metal carbonyls and find that they generally react by one of two pathways.<sup>3</sup> The anionic chains can react by simple substitution, donating electrons to a neutral metal center to form molecules such as  $[\text{M}(\text{CO})_4\text{Te}_4]^{2-}$  ( $\text{M} = \text{Cr}, \text{Mo}, \text{W}$ ),<sup>4a</sup>  $[\{\text{Cr}(\text{CO})_5\}_4\text{Te}_2]^{2-}$ ,<sup>4b</sup> and  $[\{\text{Cr}(\text{CO})_5\}_4\text{Te}_3]^{2-}$ .<sup>4b</sup> Alternatively the polychalcogenides can induce oxidation of the low-valent metal center to form higher valent metal chalcogenide complexes such as  $\text{ME}_4^{2-}$  ( $\text{M} = \text{Mo}, \text{W}$ ;  $\text{E} = \text{S}, \text{Se}$ ).<sup>5</sup> The polytellurides, because of their larger size and more metallic character, do not induce oxidative decarbonylation of metal carbonyls as readily as the polysulfides and selenides. Thus, polytellurides often react with metal carbonyls to afford clusterification products containing metal centers that have been

only partially oxidized, such as  $[\{\text{W}(\text{CO})_3\}_6(\text{Te}_2)_4]^{2-6}$  and  $[\text{Fe}_8\text{Te}_{10}(\text{CO})_{20}]^{2-}$ .<sup>7a</sup>

Because of the extensive redox chemistry displayed by iron carbonyl in the presence of polytellurides,<sup>7</sup> we have begun a more in depth investigation of the chemistry of iron carbonyl tellurides. The chemistry of the iron chalcogenides in general is very rich. Iron sulfides have received considerable attention because of their significance in living systems,<sup>8</sup> and several iron selenides and tellurides have also been reported.<sup>9</sup> Extensive work has been done with the neutral iron carbonyl telluride clusters  $\text{Fe}_3(\text{CO})_n\text{Te}_2$  ( $n = 9, 10$ ) and  $\text{Fe}_2(\text{CO})_6\text{Te}_2$ . They were first prepared by Hieber and co-workers in the mid-1950s,<sup>10</sup> and their structures and chemical behavior were thoroughly examined much later.<sup>11</sup>

\* Abstract published in *Advance ACS Abstracts*, November 15, 1994.

- (1) (a) Ansari, M. A.; Ibers, J. A. *Coord. Chem. Rev.* **1990**, *100*, 223. (b) Compton, N. A.; Errington, R. J.; Norman, N. C. *Adv. Organomet. Chem.* **1990**, *31*, 91. (c) Kanatzidis, M. G. *Comm. Inorg. Chem.* **1990**, *10*, 161. (d) Roof, L. C.; Kolis, J. W. *Chem. Rev.* **1993**, *93*, 1037.
- (2) (a) Whitmire, K. H. *J. Coord. Chem.* **1988**, *17*, 95. (b) Haushalter, R. C.; O'Conner, C. M.; Haushalter, J. P.; Umarji, A. M.; Shenoy, G. K. *Angew. Chem., Int. Ed. Engl.* **1984**, *23*, 169. (c) Steigerwald, M. L. *Chem. Mater.* **1989**, *1*, 52.
- (3) Kolis, J. W. *Coord. Chem. Rev.* **1990**, *105*, 195.
- (4) (a) Flomer, W. A.; O'Neal, S. C.; Kolis, J. W.; Jeter, D.; Cordes, A. W. *Inorg. Chem.* **1988**, *27*, 969. (b) Roof, L. C.; Pennington, W. T.; Kolis, J. W. *Inorg. Chem.* **1992**, *31*, 2056.
- (5) O'Neal, S. C.; Kolis, J. W. *J. Am. Chem. Soc.* **1988**, *110*, 1971.

(6) Roof, L. C.; Pennington, W. T.; Kolis, J. W. *J. Am. Chem. Soc.* **1990**, *112*, 8172.

(7) (a) Roof, L. C.; Pennington, W. T.; Kolis, J. W. *Angew. Chem., Int. Ed. Engl.* **1992**, *30*, 913. (b) Roof, L. C.; Pennington, W. T.; Kolis, J. W. Manuscript in preparation.

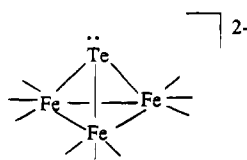
(8) Holm, R. H.; Ciurli, S.; Weigel, J. A. *Prog. Inorg. Chem.* **1990**, *38*, 1.

(9) (a) Strasdeit, H.; Krebs, B.; Henkel, G. *Inorg. Chim. Acta* **1984**, *89*, L11. (b) Bronger, W.; Kimpel, M.; Schmit, D. *Angew. Chem., Int. Ed. Engl.* **1982**, *21*, 544. (c) Steigerwald, M. L.; Siegrist, T.; Stuczynski, S. M.; Kwon, Y.-U. *J. Am. Chem. Soc.* **1992**, *114*, 3155. (d) You, J.-F.; Holm, R. H. *Inorg. Chem.* **1991**, *30*, 1431. (e) Eichhorn, B. W.; Haushalter, R. C.; Merola, J. S. *Inorg. Chem.* **1990**, *29*, 728.

(10) Hieber, W.; Gruber, J. Z. *Anorg. Allg. Chem.* **1958**, *296*, 91.

(11) (a) Schumann, H.; Magerstadt, M.; Pickardt, J. *J. Organomet. Chem.* **1982**, *240*, 407. (b) Cetini, G.; Stanghellini, P. L.; Rosetti, R.; Gambino, O. *J. Organomet. Chem.* **1968**, *15*, 373. (c) Bogan, L. E.; Lesch, D. A.; Rauchfuss, T. B. *J. Organomet. Chem.* **1983**, *250*, 429. (d) Lesch, D. A.; Rauchfuss, T. B. *Inorg. Chem.* **1981**, *20*, 3583. (e) Day, V. W.; Lesch, D. A.; Rauchfuss, T. B. *J. Am. Chem. Soc.* **1982**, *104*, 1290. (f) Mathur, P.; Mavunkal, I. J.; Rugmini, V.; Mahon, M. F. *Inorg. Chem.* **1990**, *29*, 4838. (g) Bachman, R. E.; Whitmire, K. H. *Organometallics* **1993**, *12*, 1988.

The reactions of polytellurides with iron pentacarbonyl have proven to be very complex, and a variety of products have been isolated. The products are dependent upon the nature of the polytelluride source and the stoichiometry of the reaction. When longer chain polytellurides, such as  $K_2Te_4$ , react with  $Fe(CO)_5$ , oxidative decarbonylation products form. The anionic clusters  $[Fe_5Te_4(CO)_{14}]^{2-}$ ,<sup>7a</sup>  $[Fe_8Te_{10}(CO)_{20}]^{2-}$ ,<sup>7a</sup> and  $[Fe_6Te_6(CO)_{16}]^{2-}$ <sup>7b</sup> have been isolated by this route. However, the monotelluride  $Te^{2-}$  contains no Te-Te bonds and, hence, cannot oxidize a metal center. Thus we found that  $Te^{2-}$  reacts with  $Fe(CO)_5$  to form the nonoxidized clusterification product  $[Fe_3(CO)_9Te]^{2-}$  (I) in excellent yield. This compound was also recently isolated and characterized as its bis(triphenylphosphine)nitrogen(1+) salt.<sup>12</sup> Compound I can be viewed as having  $Te^{2-}$  donating an electron pair to each iron, leaving the apical tellurium with a lone pair of electrons.



In an attempt to determine the effective electronic structure of this complex, we investigated the reactivity of electrophiles and oxidants toward the lone pair of electrons on the apical tellurium atoms. In this paper we report a convenient, high-yield synthesis and characterization of  $[(C_6H_5)_4P]_2[Fe_3(CO)_9Te]$  (I) and its reactions with a variety of hard and soft electrophiles and oxidizing agents, as well as the crystal structures of  $[PPh_3AuFe_3(CO)_9Te]^-$  (II),  $[Fe(CO)_4]_4Te]^{2-}$  (III), and  $[Fe_3(CO)_9Te_2]^-$  (IV). These reactions suggest strongly that the apical tellurium atom is unreactive toward electrophiles.

## Experimental Section

The polytelluride anions are extremely air sensitive in solution and were handled under purified argon under rigorously anaerobic conditions, using standard Schlenk techniques. All solvents were of the highest available grade and were distilled from appropriate drying agents, bubbled thoroughly with argon, and stored over activated sieves. All solids were handled in a Vacuum Atmospheres glovebox under argon. The metal carbonyls and other fine chemicals were purchased from commercial houses and used as received. The protonation reactions were carried out in  $CDCl_3$  that had been passed down a column of alumina and thoroughly degassed. All NMR spectra were obtained on a Bruker AC300. The  $^{125}Te$  NMR were obtained in sealed 10 mm tubes, in DMF with 0.5 mL of  $CD_3CN$  added to obtain lock. The spectra were referenced to an external sample of 1 M  $Te(OH)_6$  in  $D_2O$ , and shifts are reported relative to  $\delta(Me_7Te) = 0$  ppm by adding 712 to our measured values. Elemental analyses were performed by Atlantic Microlabs, Norcross, GA, and Galbraith Laboratories, Knoxville, TN.

**Preparation of  $[(C_6H_5)_4P]_2[Fe_3(CO)_9(\mu_3-Te)]$  (I).** A solution of  $K_2Te$  was prepared by stirring K (0.38 g, 9.72 mmol) and Te (0.62 g, 4.86 mmol) in DMF (20 mL) for 8 h. Three equivalents of  $Fe(CO)_5$  (1.92 mL, 14.5 mmol) was added, and the solution was stirred at 90 °C under static vacuum for 24 h. The brown solution was treated with  $PPh_3$  (4.05 g, 9.7 mmol), the resultant mixture was filtered, and the filtrate was layered with ether (20 mL). Overnight storage at 4 °C produced a tan powder, which was removed by filtration. The solvent was removed under vacuum, and the resultant dark oil was redissolved in  $CH_2Cl_2$  (25 mL). Layering with ether (10 mL) and overnight storage at room temperature produced a batch of red crystals, which were isolated by filtration. Subsequent layering of the mother liquor with ether (10 mL) produced another crop of product for a 95% total yield. IR,  $CH_2Cl_2$  solution ( $cm^{-1}$ ):  $\nu(CO) = 1991$  (w), 1923 (s), 1896 (m),

1867 (w). Anal. Calcd for  $C_{57}H_{40}Fe_3O_9P_2Te$ : C, 53.14; H, 3.23. Found: C, 53.36; H, 2.99.  $^{125}Te$  NMR ( $CD_3CN$ )  $\delta = 361.0$ .

**Protonation of  $[Fe_3(CO)_9(\mu_3-Te)]^{2-}$ .** A sample of I (0.05 g, 0.041 mmol) was placed in a flask and stirred in  $CDCl_3$  (1.5 mL) to produce a slurry. Upon addition of 1 equiv of  $CF_3SO_3H$  (3.5 mL, 0.04 mmol), the solid began to dissolve. The red solution was filtered to remove undissolved solid, and the filtrate was transferred by syringe into a 5 mm NMR tube. The  $^1H$  NMR spectrum revealed one singlet at -22.0 ppm. A second equivalent of  $CF_3SO_3H$  (3.5 mL, 0.04 mmol) was added directly to the NMR sample. A second  $^1H$  NMR spectrum showed a decrease of the resonance at -22 ppm with formation of a peak at -23.6 ppm. Layering the  $CDCl_3$  solutions of either the monoanion or the neutral cluster with ether invariably produced an amorphous powder, and crystalline product was never isolated.

**Reaction of  $[(C_6H_5)_4P]_2[Fe_3(CO)_9Te]$  with  $NOBF_4$ .** A sample of I (0.300 g, 0.245 mmol) was dissolved in  $CH_2Cl_2$  (5 mL). The red solution was transferred by syringe into a flask containing 1 equiv of  $NOBF_4$  (0.029 g, 0.25 mmol). The solution bubbled and changed color to lighter red immediately. A solution IR spectrum of the reaction mixture showed stretches at 2044 (s), 2023 (s), 1991 (s), 1969 (m), 1884 (w), 1809 (w), 1761 (m), and 1713 (vs)  $cm^{-1}$ . The solution was layered with ether (5 mL). Overnight storage at 4 °C produced a light red powder which could be redissolved in  $CH_2Cl_2$  to give a solution IR spectrum identical to that of the original reaction mixture.

**Synthesis of  $[(C_6H_5)_4P]_2[(PPh_3)AuFe_3(CO)_9Te]$  (II).** A sample of I (0.2 g, 0.16 mmol) and 1 equiv of  $(PPh_3)AuCl$  (0.081 g, 0.16 mmol) were dissolved in  $CH_2Cl_2$  (5 mL). The solution was stirred at room temperature for 0.5 h, and a color change from red to brown occurred. The solution was filtered, and the filtrate was layered with ether (5 mL). Overnight storage at 4 °C produced brown octahedral shaped crystals. Yield: 27%. IR,  $CH_2Cl_2$  solution ( $cm^{-1}$ ):  $\nu(CO) = 2016$  (s), 1962 (s), 1931 (sh, m). Anal. Calcd for  $C_{51}H_{35}AuFe_3O_9P_2Te$ : C, 45.51; H, 2.62. Found: C, 45.32; H, 2.66.

**Reaction of  $[(C_6H_5)_4P]_2[Fe_3(CO)_9Te]$  and  $(PPh_3)AuCl$ .** A sample of I (0.10 g, 0.08 mmol) and 2 equiv of  $(PPh_3)AuCl$  (0.081 g, 0.16 mmol) were stirred at room temperature for 1 h. The solution was layered with ether (5 mL) and stored at 4 °C for 24 h. A gold mirror formed on the bottom of the flask, and the colorless solution contained an amorphous powder. Because of the instability of the product, no further work was done with this system.

**Synthesis of  $[(C_6H_5)_4P]_2[(PhHg)Fe_3(CO)_9Te]$ .** A sample of I (0.200 g, 0.16 mmol) and 1 equiv of  $PhHgOAc$  (0.055 g, 0.16 mmol) were dissolved in  $CH_2Cl_2$ , and the solution was stirred at room temperature for 0.5 h. A color change from red to brown occurred, and the solution was filtered. Layering the solution with ether (5 mL) and overnight storage at 4 °C produced dark brown crystals which were isolated by filtration. Yield: 22%. IR,  $CH_2Cl_2$  solution ( $cm^{-1}$ ):  $\nu(CO) = 2034$  (w), 2016 (m), 1985 (s), 1958 (m). Anal. Calcd for  $C_{39}H_{35}Fe_3HgO_9P_2Te$ : C, 40.23; H, 2.16. Found: C, 40.09; H, 2.07.

**Synthesis of  $[(C_6H_5)_4P]_2[Fe(CO)_4]_4(\mu_4-Te)$  (III).** In a typical reaction,  $K_2Te$  was prepared *in situ* by stirring K (0.076 g, 1.94 mmol) and Te (0.124 g, 0.97 mmol) in DMF (10 mL) for 8 h. A sample of  $Fe(CO)_5$  (0.38 mL, 2.9 mmol) was added, and the cap was removed from the flask, exposing the reaction mixture to air. The brown solution was stirred for 4–6 h (note: if the reaction is not exposed to air for a sufficient length of time,  $[Fe_3(CO)_9Te]^{2-}$  will cocrystallize along with the product; if exposed for too long, the product will also decompose), and a large amount of brown orange solid, taken to be iron oxide, formed. The solution was treated with  $PPh_4Br$  (0.3 g, 0.72 mmol), and the resultant mixture was filtered. Overnight storage at 4 °C produced a tan powder, which was removed by filtration. The solvent was removed under vacuum, and the resultant oil was dissolved in  $CH_2Cl_2$  (5 mL). Layering the solution with ether (5 mL) and overnight storage at 4 °C produced dark purple crystals, which were isolated by filtration. Yield: 8%. IR,  $CH_2Cl_2$  solution ( $cm^{-1}$ ):  $\nu(CO) = 2006$  (s), 1936 (m), 1921 (s). Anal. Calcd for  $C_{64}H_{40}Fe_4O_{16}P_2Te$ : C, 52.01; H, 2.73. Found: C, 51.09; H, 2.73.

**Synthesis of  $[(C_6H_5)_4P]_2[Fe_3Te_2(CO)_9]^-$  (IV).** A sample of I (0.3 g, 0.24 mmol) and 1 equiv of  $I_2$  (0.062 g, 0.24 mmol) were stirred in  $CH_2Cl_2$  (5 mL) for 2 h, until the IR spectrum in the CO region for the starting material changed completely. The dark red solution was layered with ether (5 mL) and stored at 4 °C for 8 h. A colorless solid formed,

(12) Bachman, R. E.; Whitmire, K. H. *Inorg. Chem.* **1994**, *33*, 2527.

Table 1. Crystallographic Data

	I	II	III	IV
formula	C <sub>57</sub> H <sub>40</sub> O <sub>9</sub> P <sub>2</sub> Fe <sub>3</sub> Te	C <sub>51</sub> H <sub>35</sub> O <sub>9</sub> P <sub>2</sub> Fe <sub>3</sub> TeAu	C <sub>64</sub> H <sub>40</sub> O <sub>16</sub> P <sub>2</sub> Fe <sub>4</sub> Te	C <sub>33</sub> H <sub>20</sub> O <sub>9</sub> PFe <sub>3</sub> TeI
fw	1226.03	1345.89	1477.9	1141.11
space group	P2 <sub>1</sub> /n	P2 <sub>1</sub> /c	C2/c	P $\bar{1}$
a, Å	11.034(3)	16.970(5)	14.264(4)	9.614(1)
b, Å	22.214(8)	13.996(4)	19.719(5)	14.511(2)
c, Å	21.980(8)	21.108(8)	22.937(10)	14.668(2)
$\alpha$ , deg				74.47(1)
$\beta$ , deg	97.72(3)	95.25(3)	90.55(3)	71.14(1)
$\gamma$ , deg				83.22(1)
V, Å <sup>3</sup>	5339(3)	4992(3)	6451(3)	1852.7(5)
Z	4	4	4	2
$\rho_{\text{calcd}}$ , g cm <sup>-3</sup>	1.52	1.79	1.52	2.03
$\mu$ (Mo K $\alpha$ ), mm <sup>-1</sup>	1.45	4.47	1.44	3.61
transm coeff	0.82–1.00	0.71–1.00	0.58–1.00	0.46–1.00
R <sup>a</sup>	0.0819	0.0507	0.0454	0.0398
R <sub>w</sub> <sup>b</sup>	0.097	0.0579	0.0524	0.0542

$$^a R = \sum |F_o| - |F_c| / \sum |F_o|, \quad ^b R_w = [\sum w(|F_o| - |F_c|)^2 / \sum w|F_o|^2]^{1/2}; \quad w = 1/[\sigma^2(F_o) + gF_o^2].$$

Table 2. Selected Atomic Coordinates ( $\times 10^4$ ) and Equivalent Isotropic Displacement Coefficients ( $\text{Å}^2 \times 10^3$ ) for I

Te(1)	x	y	z	U <sub>eq</sub> <sup>a</sup>
Te(1)	917(1)	3192(1)	7998(1)	59(1)
Fe(1)	73(2)	2321(1)	7359(1)	43(1)
Fe(2)	-571(2)	2534(1)	8450(1)	45(1)
Fe(3)	-1273(2)	3264(1)	7539(1)	41(1)
Fe(1a)	-422(41)	2737(21)	7105(19)	61(13)
Fe(2a)	103(49)	2214(24)	8250(22)	77(16)
Fe(3a)	-1138(52)	3142(26)	8016(27)	87(17)
O(1)	-2119(14)	1785(8)	6674(7)	95(7)
O(2)	1349(16)	2606(7)	6317(7)	100(7)
O(3)	1404(18)	1255(9)	7848(8)	120(9)
O(4)	-2106(12)	1495(6)	8120(6)	66(5)
O(5)	1018(15)	1944(11)	9417(8)	134(10)
O(6)	-2044(14)	3247(7)	9192(6)	87(6)
O(7)	-1890(16)	4422(7)	8016(7)	98(8)
O(8)	-3654(12)	2704(6)	7564(6)	62(5)
O(9)	-1429(14)	3555(8)	6235(6)	88(7)
C(1)	-1240(20)	2013(8)	6958(9)	59(8)
C(2)	816(21)	2504(9)	6720(9)	72(9)
C(3)	864(22)	1683(12)	7663(10)	90(11)
C(4)	-1469(15)	1905(9)	8230(7)	46(6)
C(5)	423(18)	2189(11)	9013(9)	72(9)
C(6)	-1458(19)	2960(8)	8893(9)	60(7)
C(7)	-1644(18)	3947(9)	7839(8)	57(7)
C(8)	-2695(18)	2906(7)	7571(8)	46(7)
C(9)	-1314(18)	3434(9)	6749(9)	63(8)

<sup>a</sup> Equivalent isotropic  $U$  defined as one-third of the trace of the orthogonalized  $U_{ij}$  tensor. Atoms Fe(1a)–Fe(3a) represent alternative positions ( $m = 0.067$ ) for the iron atoms Fe(1)–Fe(3).

which was removed by filtration. Treating the solution with a second aliquot of ether (5 mL) and overnight storage at 4 °C produced red rod-shaped crystals which were isolated by filtration. Yield: 20%. IR, CH<sub>2</sub>Cl<sub>2</sub> solution (cm<sup>-1</sup>):  $\nu(\text{CO}) = 2063$  (w), 2045 (m), 2029 (s), 2005 (s), 1987 (m, sh), 1960 (m).

**Reaction of [(C<sub>6</sub>H<sub>5</sub>)<sub>4</sub>P]<sub>2</sub>[Fe<sub>3</sub>(CO)<sub>9</sub>Te] and AgNO<sub>3</sub>.** Several reactions were carried out with [Fe<sub>3</sub>(CO)<sub>9</sub>Te]<sup>2-</sup> and AgNO<sub>3</sub> in a variety of solvents (CH<sub>2</sub>Cl<sub>2</sub>, CH<sub>3</sub>CN, THF, DMF) and stoichiometries, but only amorphous powders could be isolated. Judging from the drastic changes in the CO region of the IR upon varying the solvent, the products appear to be very sensitive, and reactive. The cleanest solution IR was obtained when 3 equiv of AgNO<sub>3</sub> was reacted with [Fe<sub>3</sub>(CO)<sub>9</sub>Te]<sup>2-</sup> in CH<sub>2</sub>Cl<sub>2</sub>, although only amorphous powders were isolated. IR, CH<sub>2</sub>Cl<sub>2</sub> solution (cm<sup>-1</sup>):  $\nu(\text{CO}) = 2047$  (s), 2024 (s), 1998 (s), 1964 (w).

**X-ray Structure Analyses.** Intensity measurements were made at room temperature (21 °C) on a Nicolet R3mV diffractometer with graphite-monochromated Mo K $\alpha$  radiation ( $\lambda = 0.71073$  Å). Relevant crystallographic data are given in Table 1. Data were measured to  $2\theta = 45^\circ$  ( $50^\circ$  for IV) using  $\omega/2\theta$  scans at speeds of 2–15°/min (in  $\omega$ ). Periodic measurement of three standard reflections indicated crystal and electronic stability ( $\pm 2\%$ ) for all compounds. Lorentz and

Table 3. Selected Atomic Coordinates ( $\times 10^4$ ) and Equivalent Isotropic Displacement Coefficients ( $\text{Å}^2 \times 10^3$ ) for II

	x	y	z	U <sub>eq</sub> <sup>a</sup>
Au(1)	2976(1)	3897(1)	3074(1)	48(1)
Te(1)	1058(1)	2082(1)	3452(1)	67(1)
Fe(1)	1681(1)	3678(2)	3699(1)	47(1)
Fe(2)	2449(1)	2121(2)	3153(1)	50(1)
Fe(3)	2102(2)	2128(2)	4339(1)	60(1)
P(1)	3866(2)	4936(3)	2700(2)	41(1)
O(1)	2760(8)	5032(11)	4371(7)	97(6)
O(2)	899(8)	4755(12)	2633(7)	106(7)
O(3)	528(7)	4210(9)	4564(6)	76(5)
O(4)	4147(8)	2093(11)	3457(9)	124(8)
O(5)	2209(10)	2427(11)	1787(7)	114(8)
O(6)	2427(13)	57(10)	3055(9)	146(10)
O(7)	3506(12)	2974(11)	4798(8)	123(8)
O(8)	1188(13)	2458(13)	5411(8)	148(10)
O(9)	2584(11)	135(10)	4608(7)	119(8)
C(1)	2368(11)	4462(14)	4071(9)	64(5)
C(2)	1222(11)	4319(13)	3020(9)	62(5)
C(3)	972(10)	3983(14)	4222(9)	61(5)
C(4)	3435(12)	2172(13)	3355(9)	67(5)
C(5)	2295(10)	2328(13)	2332(9)	60(5)
C(6)	2434(13)	884(16)	3106(10)	85(7)
C(7)	2992(6)	2683(8)	4579(5)	2(3)
C(8)	1583(13)	2329(16)	4996(11)	87(7)
C(9)	2374(12)	889(16)	4502(10)	80(6)
C(11)	3509(9)	6153(12)	2658(7)	45(4)
C(12)	2685(10)	6291(13)	2579(8)	63(5)
C(13)	2355(14)	7216(16)	2551(10)	95(7)
C(14)	2836(13)	7912(17)	2593(10)	92(7)
C(15)	3628(14)	7894(17)	2645(11)	103(8)
C(16)	3991(12)	4650(10)	1900(7)	40(4)
C(22)	4060(10)	3681(12)	1722(8)	60(5)
C(23)	4194(11)	3395(15)	1111(10)	76(6)
C(24)	4339(11)	4071(15)	671(10)	81(6)
C(25)	4397(11)	5033(15)	824(10)	78(6)
C(26)	4262(9)	5306(13)	1456(8)	58(5)
C(31)	4802(8)	5075(10)	3161(7)	37(4)
C(32)	4806(10)	5109(12)	3820(8)	61(5)
C(33)	5495(10)	5320(12)	4202(9)	65(5)
C(34)	6192(11)	5455(12)	3936(9)	64(5)
C(35)	6219(11)	5366(13)	3297(9)	68(5)
C(36)	5525(10)	5188(12)	2901(9)	60(5)

<sup>a</sup> Equivalent isotropic  $U$  defined as one-third of the trace of the orthogonalized  $U_{ij}$  tensor.

polarization corrections and an empirical absorption correction ( $\psi$  scan) were applied to the data for each compound.

The structures were solved by direct methods and refined by full-matrix least-squares techniques using the SHELXTL-Plus package of programs. All non-hydrogen atoms were refined anisotropically (the carbon atoms of II were refined isotropically). Hydrogen atoms were included in the structure factor calculation for each compound at

**Table 4.** Selected Atomic Coordinates ( $\times 10^4$ ) and Equivalent Isotropic Displacement Coefficients ( $\text{\AA}^2 \times 10^3$ ) for **III**

	<i>x</i>	<i>y</i>	<i>z</i>	$U_{\text{eq}}^a$
Te(1)	0	3582(1)	2500	41(1)
Fe(1)	-1361(1)	2806(1)	2905(1)	48(1)
Fe(2)	-637(1)	4350(1)	1645(1)	60(1)
O(1)	-2862(5)	1934(4)	3323(4)	104(4)
O(2)	-321(5)	2631(4)	4005(4)	83(3)
O(3)	-1113(5)	1859(3)	1933(4)	87(3)
O(4)	-2741(5)	3902(4)	2775(4)	96(3)
O(5)	-1321(8)	5176(5)	702(5)	165(6)
O(6)	-1390(5)	5336(4)	2467(4)	115(4)
O(7)	1273(6)	4554(4)	1207(5)	119(4)
O(8)	-1833(5)	3249(3)	1205(4)	88(3)
C(1)	-2261(7)	2281(5)	3168(5)	64(4)
C(2)	-697(6)	2706(5)	3570(6)	59(4)
C(3)	-1187(6)	2247(4)	2305(5)	58(4)
C(4)	-2161(6)	3492(5)	2823(4)	62(4)
C(55)	-1050(8)	4845(5)	1071(7)	99(5)
C(6)	-1081(7)	4938(5)	2157(6)	84(6)
C(7)	533(8)	4458(5)	1395(5)	78(5)
C(8)	-1334(6)	3658(4)	1396(4)	57(4)

<sup>a</sup> Equivalent isotropic  $U$  defined as one-third of the trace of the orthogonalized  $U_{ij}$  tensor.

**Table 5.** Selected Atomic Coordinates ( $\times 10^4$ ) and Equivalent Isotropic Displacement Coefficients ( $\text{\AA}^2 \times 10^3$ ) for **IV**

	<i>x</i>	<i>y</i>	<i>z</i>	$U_{\text{eq}}^a$
I(1)	1572(1)	1582(1)	5285(1)	59(1)
Te(1)	2572(1)	2274(1)	7373(1)	41(1)
Te(2)	2362(1)	4500(1)	6517(1)	51(1)
Fe(1)	1817(1)	3187(1)	5770(1)	44(1)
Fe(2)	1570(1)	3586(1)	8349(1)	52(1)
Fe(3)	4316(1)	3529(1)	7274(1)	49(1)
O(1)	987(8)	4487(5)	4113(4)	103(3)
O(2)	4877(6)	3204(5)	4489(4)	80(3)
O(3)	-1260(6)	2943(6)	7032(5)	105(4)
O(4)	1724(11)	5270(5)	9036(5)	121(4)
O(5)	1618(8)	2327(5)	10256(4)	89(3)
O(6)	-1635(7)	3704(6)	8808(5)	101(3)
O(7)	5169(10)	5237(5)	7635(6)	120(5)
O(8)	5473(7)	2112(4)	8706(4)	82(3)
O(9)	6920(6)	3460(5)	5566(5)	91(3)
C(1)	1319(8)	3972(6)	4759(5)	62(3)
C(2)	3727(7)	3197(5)	5006(5)	52(3)
C(3)	-80(8)	3061(6)	6561(6)	65(3)
C(4)	1702(11)	4619(6)	8746(6)	78(4)
C(5)	1632(9)	2806(5)	9493(5)	60(3)
C(6)	-383(9)	3634(6)	8600(6)	68(3)
C(7)	4823(10)	4569(7)	7500(7)	79(4)
C(8)	5016(8)	2675(5)	8157(5)	58(3)
C(9)	5866(8)	3485(6)	6204(5)	62(3)

<sup>a</sup> Equivalent isotropic  $U$  defined as one-third of the trace of the orthogonalized  $U_{ij}$  tensor.

optimized positions ( $d_{\text{C-H}} = 0.96 \text{ \AA}$ ) with a refined group thermal parameter ( $U_{\text{H}}$ : 0.08(1)  $\text{\AA}^2$  for **I**, 0.11(1)  $\text{\AA}^2$  for **II**, 0.095(8)  $\text{\AA}^2$  for **III**, 0.085(6)  $\text{\AA}^2$  for **IV**). The iron atoms of **I** are disordered over two possible sets of positions related by a 44(1) $^\circ$  rotation about the normal to the iron plane. Refinement of an occupancy factor in the early stages gave  $m = 0.067$  for the minor site; this factor was constrained in the latter stages of refinement. The light atoms associated with the minor site could not be located. The anion of compound **III** possesses crystallographic 2-fold symmetry; in the other three compounds the anions occupy general positions. Positional parameters of the anions are given in Tables 2–5 for compounds **I** through **IV**, respectively. Selected distances and angles are listed in Tables 6–9 for the four compounds.

## Discussion

**Structure and Bonding of  $[(\text{C}_6\text{H}_5)_4\text{P}]_2[\{\text{Fe}(\text{CO})_3\}_3(\mu_3\text{-Te})]$  (**I**).** The structure of **I** has been determined by single-crystal

**Table 6.** Selected Bond Distances ( $\text{\AA}$ ) and Angles (deg) for **I**

Distances			
Te(1)–Fe(1)	2.495(3)	Te(1)–Fe(2)	2.501(3)
Te(1)–Fe(3)	2.496(3)	Fe(1)–Fe(2)	2.634(4)
Fe(1)–Fe(3)	2.630(4)	Fe(1)–C(1)	1.732(20)
Fe(1)–C(2)	1.766(22)	Fe(1)–C(3)	1.749(26)
Fe(2)–Fe(3)	2.612(4)	Fe(2)–C(4)	1.744(19)
Fe(2)–C(5)	1.719(20)	Fe(2)–C(6)	1.748(21)
Fe(3)–C(7)	1.724(19)	Fe(3)–C(8)	1.769(20)
Fe(3)–C(9)	1.773(19)	O(1)–C(1)	1.194(25)
O(2)–C(2)	1.150(28)	O(3)–C(3)	1.166(32)
O(4)–C(4)	1.157(23)	O(5)–C(5)	1.166(27)
O(6)–C(6)	1.171(26)	O(7)–C(7)	1.169(25)
O(8)–C(8)	1.147(23)	O(9)–C(9)	1.150(24)
Te(1)–Fe(1a)	2.505(42)	Te(1)–Fe(3a)	2.276(58)
Te(1)–Fe(2a)	2.441(53)	Fe(1a)–Fe(2a)	2.762(64)
Fe(1a)–Fe(3a)	2.422(76)	Fe(2a)–Fe(3a)	2.489(77)
Angles			
Fe(1)–Te(1)–Fe(2)	63.6(1)	Fe(1)–Te(1)–Fe(3)	63.6(1)
Fe(2)–Te(1)–Fe(3)	63.0(1)	Te(1)–Fe(1)–Fe(2)	58.3(1)
Te(1)–Fe(1)–Fe(3)	58.2(1)	Fe(2)–Fe(1)–Fe(3)	59.5(1)
Te(1)–Fe(1)–C(1)	144.6(7)	Te(1)–Fe(1)–C(2)	95.2(6)
Te(1)–Fe(1)–C(3)	106.5(8)	Fe(2)–Fe(1)–C(1)	103.0(7)
Fe(2)–Fe(1)–C(2)	153.3(6)	Fe(2)–Fe(1)–C(3)	88.8(8)
Fe(3)–Fe(1)–C(1)	86.6(7)	Fe(3)–Fe(1)–C(2)	105.6(7)
Fe(3)–Fe(1)–C(3)	148.3(8)	C(1)–Fe(1)–C(2)	97.6(9)
C(1)–Fe(1)–C(3)	102.4(10)	C(2)–Fe(1)–C(3)	103.2(11)
Te(1)–Fe(2)–Fe(1)	58.1(1)	Te(1)–Fe(2)–Fe(3)	58.4(1)
Fe(1)–Fe(2)–Fe(3)	60.2(1)	Te(1)–Fe(2)–C(4)	137.4(6)
Te(1)–Fe(2)–C(5)	99.0(7)	Te(1)–Fe(2)–C(6)	110.6(7)
Fe(1)–Fe(2)–C(4)	79.4(6)	Fe(1)–Fe(2)–C(5)	110.5(7)
Fe(1)–Fe(2)–C(6)	147.6(6)	Fe(3)–Fe(2)–C(4)	100.7(5)
Fe(3)–Fe(2)–C(5)	157.4(8)	Fe(3)–Fe(2)–C(6)	87.7(6)
C(4)–Fe(2)–C(5)	97.2(10)	C(4)–Fe(2)–C(6)	104.4(9)
C(5)–Fe(2)–C(6)	101.0(10)	Te(1)–Fe(3)–Fe(1)	58.2(1)
Te(1)–Fe(3)–Fe(2)	58.6(1)	Fe(1)–Fe(3)–Fe(2)	60.3(1)
Te(1)–Fe(3)–C(7)	99.8(6)	Te(1)–Fe(3)–C(8)	140.4(5)
Te(1)–Fe(3)–C(9)	107.8(7)	Fe(1)–Fe(3)–C(7)	157.9(6)
Fe(1)–Fe(3)–C(8)	99.8(5)	Fe(1)–Fe(3)–C(9)	87.8(7)
Fe(2)–Fe(3)–C(7)	108.4(6)	Fe(2)–Fe(3)–C(8)	82.2(5)
Fe(2)–Fe(3)–C(9)	148.1(7)	C(7)–Fe(3)–C(8)	97.1(9)
C(7)–Fe(3)–C(9)	102.2(9)	C(8)–Fe(3)–C(9)	103.2(8)
Fe(1)–C(1)–O(1)	177.6(17)	Fe(1)–C(2)–O(2)	176.6(18)
Fe(1)–C(3)–O(3)	177.9(22)	Fe(2)–C(4)–O(4)	175.2(16)
Fe(2)–C(5)–O(5)	174.7(20)	Fe(2)–C(6)–O(6)	179.5(20)
Te(1)–C(7)–O(7)	176.9(18)	Fe(3)–C(8)–O(8)	175.2(14)
Fe(3)–C(9)–O(9)	175.0(19)	Fe(1a)–Te(1)–Fe(2a)	67.9(15)
Fe(1a)–Te(1)–Fe(3a)	60.6(18)	Fe(2a)–Te(1)–Fe(3a)	63.6(19)
Te(1)–Fe(1a)–Fe(2a)	55.0(13)	Te(1)–Fe(1a)–Fe(3a)	55.0(16)
Fe(2a)–Fe(1a)–Fe(3a)	56.9(20)	Te(1)–Fe(2a)–Fe(1a)	57.2(14)
Te(1)–Fe(2a)–Fe(3a)	55.0(17)	Fe(1a)–Fe(2a)–Fe(3a)	54.6(20)
Te(1)–Fe(3a)–Fe(1a)	64.4(19)	Te(1)–Fe(3a)–Fe(2a)	61.5(19)
Fe(1a)–Fe(3a)–Fe(2a)	68.4(22)		

X-ray diffraction and consists of two well-separated tetraphenylphosphonium cations, and a  $[\text{Fe}_3(\text{CO})_9\text{Te}]^{2-}$  dianion containing a  $\text{Fe}_3(\text{CO})_9$  fragment capped by a telluride (Figure 1). The structure of the anionic cluster is nearly identical to that reported earlier using a different counterion.<sup>12</sup> The compound can be formally envisioned as a neutral triiron fragment and a  $(\mu_3\text{-Te})^{2-}$  ion donating an electron pair to each  $\text{Fe}(\text{CO})_3$  vertex, with the telluride retaining one lone pair of electrons. The Fe–Fe bonds range from 2.612(4) to 2.634(4)  $\text{\AA}$ , which are considered normal, as are the Fe–Te bonds, which range from 2.495(3) to 2.501(3)  $\text{\AA}$  (see Table 6). The similarity of the Fe–Fe bonds to the Fe–Te bonds makes the molecule nearly a perfect tetrahedron, with the Fe–Te–Fe angles averaging 63.4(1) $^\circ$ . The Fe–Te–Fe angles are probably slightly wider due to the larger telluride vertex. Each iron contains three terminal CO ligands, with Fe–C–O angles averaging 177(2) $^\circ$  and C–Fe–C angles averaging 101(9) $^\circ$ . The Fe–C and C–O bond distances are typical, averaging 1.75(2) and 1.16(3)  $\text{\AA}$ , respectively. This

Table 7. Selected Bond Distances (Å) and Angles (deg) for II

				Distances			
Au(1)–Fe(1)	2.681(3)	Au(1)–Fe(2)	2.652(3)	O(4)–C(4)	1.213(24)	O(5)–C(5)	1.154(24)
Au(1)–P(1)	2.290(4)	Te(1)–Fe(1)	2.505(3)	O(6)–C(6)	1.162(27)	O(7)–C(7)	1.032(21)
Te(1)–Fe(2)	2.499(3)	Te(1)–Fe(3)	2.457(3)	O(8)–C(8)	1.165(31)	O(9)–C(9)	1.131(26)
Fe(1)–Fe(2)	2.836(3)	Fe(1)–Fe(3)	2.620(3)	C(11)–C(12)	1.406(22)	C(11)–C(16)	1.383(26)
Fe(1)–C(1)	1.736(18)	Fe(1)–C(2)	1.806(19)	C(12)–C(13)	1.409(29)	C(13)–C(14)	1.269(32)
Fe(1)–C(3)	1.759(19)	Fe(2)–Fe(3)	2.622(4)	C(14)–C(15)	1.339(33)	C(15)–C(16)	1.457(32)
Fe(2)–C(4)	1.689(20)	Fe(2)–C(5)	1.754(20)	C(21)–C(22)	1.406(22)	C(21)–C(26)	1.361(23)
Fe(2)–C(6)	1.735(23)	Fe(3)–C(7)	1.732(11)	C(22)–C(23)	1.389(27)	C(23)–C(24)	1.363(29)
Fe(3)–C(8)	1.733(24)	Fe(3)–C(9)	1.819(22)	C(24)–C(25)	1.386(29)	C(25)–C(26)	1.427(27)
P(1)–C(11)	1.807(16)	P(1)–C(21)	1.810(16)	C(31)–C(32)	1.392(22)	C(31)–C(36)	1.397(23)
P(1)–C(31)	1.795(14)	O(1)–C(1)	1.184(23)	C(32)–C(33)	1.390(24)	C(33)–C(34)	1.367(26)
O(2)–C(2)	1.122(23)	O(3)–C(3)	1.135(23)	C(34)–C(35)	1.360(26)	C(35)–C(36)	1.403(24)
Angles							
Fe(1)–Au(1)–Fe(2)	64.3(1)	Fe(1)–Au(1)–P(1)	147.0(1)	Fe(1)–Fe(3)–C(7)	88.2(4)	Fe(2)–Fe(3)–C(7)	90.9(4)
Fe(2)–Au(1)–P(1)	148.6(1)	Fe(1)–Te(1)–Fe(2)	69.1(1)	Te(1)–Fe(3)–C(8)	103.3(7)	Fe(1)–Fe(3)–C(8)	98.3(7)
Fe(1)–Te(1)–Fe(3)	63.7(1)	Fe(2)–Te(1)–Fe(3)	63.9(1)	Fe(2)–Fe(3)–C(8)	159.9(7)	C(7)–Fe(3)–C(8)	100.7(8)
Au(1)–Fe(1)–Te(1)	110.4(1)	Au(1)–Fe(1)–Fe(2)	57.4(1)	Te(1)–Fe(3)–C(9)	105.8(7)	Fe(1)–Fe(3)–C(9)	160.0(7)
Te(1)–Fe(1)–Fe(2)	55.4(1)	Au(1)–Fe(1)–Fe(3)	98.7(1)	Fe(2)–Fe(3)–C(9)	95.9(7)	C(7)–Fe(3)–C(9)	100.0(8)
Te(1)–Fe(1)–Fe(3)	57.2(1)	Fe(2)–Fe(1)–Fe(3)	57.3(1)	C(8)–Fe(3)–C(9)	98.1(10)	Au(1)–P(1)–C(11)	112.7(5)
Au(1)–Fe(1)–C(1)	66.6(7)	Te(1)–Fe(1)–C(1)	155.7(6)	Au(1)–P(1)–C(21)	112.5(5)	C(11)–P(1)–C(21)	105.2(7)
Fe(2)–Fe(1)–C(1)	110.8(6)	Fe(3)–Fe(1)–C(1)	98.7(6)	Au(1)–P(1)–C(31)	117.4(5)	C(11)–P(1)–C(31)	101.6(7)
Au(1)–Fe(1)–C(2)	82.3(6)	Te(1)–Fe(1)–C(2)	97.8(6)	C(21)–P(1)–C(31)	106.1(7)	Fe(1)–C(1)–O(1)	171.4(18)
Fe(2)–Fe(1)–C(2)	103.9(6)	Fe(3)–Fe(1)–C(2)	153.9(6)	Fe(1)–C(2)–O(2)	174.1(18)	Fe(1)–C(3)–O(3)	177.5(18)
C(1)–Fe(1)–C(2)	105.5(9)	Au(1)–Fe(1)–C(3)	156.9(6)	Fe(2)–C(4)–O(4)	171.2(16)	Fe(2)–C(5)–O(5)	177.0(17)
Te(1)–Fe(1)–C(3)	92.7(6)	Fe(2)–Fe(1)–C(3)	143.8(6)	Fe(2)–C(6)–O(6)	178.0(21)	Fe(3)–C(7)–O(7)	170.4(14)
Fe(3)–Fe(1)–C(3)	92.7(6)	C(1)–Fe(1)–C(3)	91.9(9)	Fe(3)–C(8)–O(8)	175.4(20)	Fe(3)–C(9)–O(9)	176.2(20)
C(2)–Fe(1)–C(3)	96.1(8)	Au(1)–Fe(2)–Te(1)	111.6(1)	P(1)–C(11)–C(12)	117.4(12)	P(1)–C(11)–C(16)	124.3(13)
Au(1)–Fe(2)–Te(1)	58.4(1)	Te(1)–Fe(2)–Fe(1)	55.6(1)	C(12)–C(11)–C(16)	118.2(16)	C(11)–C(12)–C(13)	121.2(17)
Au(1)–Fe(2)–Fe(3)	99.4(1)	Te(1)–Fe(2)–Fe(3)	57.3(1)	C(12)–C(13)–C(14)	116.9(21)	C(13)–C(14)–C(15)	128.7(24)
Fe(1)–Fe(2)–Fe(3)	57.2(1)	Au(1)–Fe(2)–C(4)	69.2(6)	C(14)–C(15)–C(16)	116.0(21)	C(11)–C(16)–C(15)	118.9(19)
Te(1)–Fe(2)–C(4)	150.8(7)	Fe(1)–Fe(2)–C(4)	110.2(6)	P(1)–C(21)–C(22)	117.2(12)	P(1)–C(21)–C(26)	124.6(12)
Fe(3)–Fe(2)–C(4)	93.6(7)	Au(1)–Fe(2)–C(5)	78.7(6)	C(22)–C(21)–C(26)	118.1(15)	C(21)–C(22)–C(23)	121.4(16)
Te(1)–Fe(2)–C(5)	101.2(6)	Fe(1)–Fe(2)–C(5)	104.0(6)	C(22)–C(23)–C(24)	119.1(19)	C(23)–C(24)–C(25)	121.9(20)
Fe(3)–Fe(2)–C(5)	156.4(6)	C(4)–Fe(2)–C(5)	107.3(9)	C(24)–C(25)–C(26)	117.6(18)	C(21)–C(26)–C(25)	121.7(16)
Au(1)–Fe(2)–C(6)	159.3(8)	Te(1)–Fe(2)–C(6)	89.1(7)	P(1)–C(31)–C(32)	117.9(12)	P(1)–C(31)–C(36)	124.3(12)
Fe(1)–Fe(2)–C(6)	141.8(8)	Fe(3)–Fe(2)–C(6)	93.2(7)	C(32)–C(31)–C(36)	117.7(14)	C(31)–C(32)–C(33)	120.9(16)
C(4)–Fe(2)–C(6)	93.8(10)	C(5)–Fe(2)–C(6)	96.2(9)	C(32)–C(33)–C(34)	120.3(17)	C(33)–C(34)–C(35)	120.2(17)
Te(1)–Fe(3)–Fe(1)	59.0(1)	Te(1)–Fe(3)–Fe(2)	58.8(1)	C(34)–C(35)–C(36)	120.3(18)	C(31)–C(36)–C(35)	120.4(16)
Fe(1)–Fe(3)–Fe(2)	65.5(1)	Te(1)–Fe(3)–C(7)	141.6(4)				

type of capped cluster is well-known and is similar to [Ir<sub>3</sub>(CO)<sub>9</sub>-Bi]<sup>13</sup> and [BiFe<sub>3</sub>(CO)<sub>9</sub>(μ<sub>3</sub>-CO)]<sup>-</sup>, except for the bridging CO.<sup>14</sup> In addition, the molecules [H<sub>2</sub>M<sub>3</sub>(CO)<sub>9</sub>(μ<sub>3</sub>-E)] (M = Ru, Os; E = S, Se, Te) are all known,<sup>15</sup> as are [Fe<sub>3</sub>(CO)<sub>9</sub>E]<sup>2-</sup> (E = O, S, Se).<sup>16–18</sup>

The bonding in I is fairly straightforward and may be described similarly to that of other capped three metal clusters. There is an octet about the tellurium including one lone pair, and the 18-electron count around each iron is completed by donation of a lone pair of electrons from the telluride, with formation of the metal–metal bonds. The cluster also obeys Lauher's predictions<sup>19</sup> and can be viewed as a 48-electron closed three-metal cluster with tellurium donating 4 electrons to the cluster count while retaining a nonbonding lone pair of electrons.

**Structure and Bonding of [(C<sub>6</sub>H<sub>5</sub>)<sub>4</sub>P][[(PPh<sub>3</sub>Au)Fe<sub>3</sub>(CO)<sub>9</sub>Te] (II).** The structure of II consists of an [Fe(CO)<sub>3</sub>]<sub>3</sub> triangle which

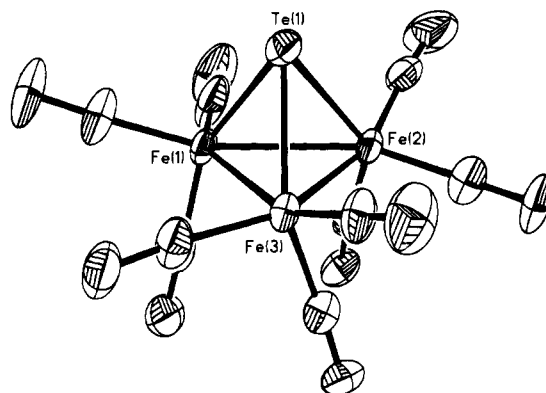


Figure 1. Thermal ellipsoid plot of [Fe<sub>3</sub>(CO)<sub>9</sub>Te]<sup>2-</sup> (I). (Ellipsoids are at 35% probability.)

is capped by a μ<sub>3</sub>-Te<sup>2-</sup> ion, with one edge bridged by a (PPh<sub>3</sub>)Au<sup>+</sup> cation (Figure 2). The (PPh<sub>3</sub>)Au<sup>+</sup> fragment is approximately evenly placed across one iron–iron bond. The Fe–Au distances of 2.681(3) and 2.652(3) Å and an Fe–Au–Fe angle of 64.3(1)° (see Table 7) are similar to those in other clusters of this type.<sup>20,21</sup> The bridged Fe(1)–Fe(2) distance is noticeably longer at 2.837(4) Å, compared to the unbridged Fe(1)–Fe(3) and Fe(2)–Fe(3) distances at 2.620(3) and 2.623(4) Å. The (PPh<sub>3</sub>)Au<sup>+</sup> ion lies below the plane of the Fe<sub>3</sub>Te tetrahedron, with an Au–Fe(1)–Fe(3) angle of 98.7(1)° and

(20) Umland, H.; Behrens, U. *J. Organomet. Chem.* **1985**, *287*, 109.

(21) Bruce, M. I.; Nicholson, B. K. *J. Organomet. Chem.* **1983**, *250*, 627.

(13) Kruppa, W.; Blaser, D.; Boese, R.; Schmid, G. *Z. Naturforsch.* **1982**, *37B*, 209.

(14) Whitmire, K. H.; Lagrone, C. B.; Churchill, M. R.; Fettingner, J. C.; Vollaro Biondi, L. *Inorg. Chem.* **1984**, *23*, 4227.

(15) Schacht, H.-T.; Powell, A. K.; Vahrenkamp, H.; Koike, M.; Kneuper, H.-J.; Shapley, J. R. *J. Organomet. Chem.* **1989**, *368*, 269 and references therein.

(16) Ceriotti, A.; Resconi, L.; Demartin, R.; Longoni, G.; Manassero, M.; Sansoni, M. *J. Organomet. Chem.* **1983**, *249*, C35.

(17) Shigui, Z.; Lixin, W.; Hengbin, Z.; Ling, Y.; Yuguo, F. *Eur. J. Solid State Inorg. Chem.* **1991**, *28*, 1269.

(18) Holliday, R. L.; Hargus, B.; Smith, D. M.; Kolis, J. W. *Polyhedron*, submitted for publication.

(19) Lauher, J. W. *J. Am. Chem. Soc.* **1979**, *101*, 2604.

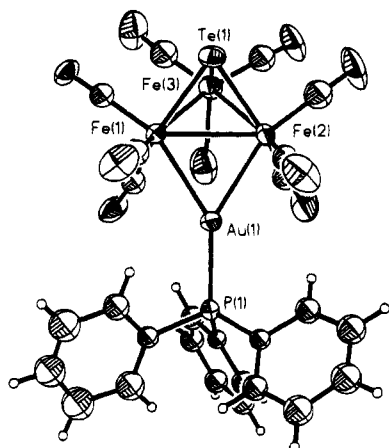


**Figure 2.** Thermal ellipsoid plot of  $[(PPh_3)AuFe_3(CO)_9]Te^-$  (**II**). (Ellipsoids are at 35% probability.)

**Table 8.** Selected Bond Distances (Å) and Angles (deg) for **III**<sup>a</sup>

Distances			
Te(1)–Fe(1)	2.647(2)	Te(1)–Fe(2)	2.634(2)
Fe(1)–C(1)	1.761(10)	Fe(1)–C(2)	1.798(11)
Fe(1)–C(3)	1.784(10)	Fe(1)–C(4)	1.778(9)
Fe(2)–C(5)	1.737(13)	Fe(2)–C(6)	1.772(12)
Fe(2)–C(7)	1.783(12)	Fe(2)–C(8)	1.779(9)
O(1)–C(1)	1.155(12)	O(2)–C(2)	1.137(14)
O(3)–C(3)	1.151(13)	O(4)–C(4)	1.162(11)
O(5)–C(5)	1.132(17)	O(6)–C(6)	1.150(14)
O(7)–C(7)	1.159(14)	O(8)–C(8)	1.159(11)
Angles			
Fe(1)–Te(1)–Fe(2)	110.2(1)	Fe(1)–Te(1)–Fe(1a)	109.4(1)
Fe(2)–Te(1)–Fe(1a)	108.7(1)	Fe(2)–Te(1)–Fe(2a)	109.7(1)
Te(1)–Fe(1)–C(1)	179.2(3)	Te(1)–Fe(1)–C(2)	88.8(3)
C(1)–Fe(1)–C(2)	91.4(4)	Te(1)–Fe(1)–C(3)	88.7(3)
C(1)–Fe(1)–C(3)	90.5(4)	C(2)–Fe(1)–C(3)	120.7(4)
Te(1)–Fe(1)–C(4)	89.7(3)	C(1)–Fe(1)–C(4)	90.8(4)
C(2)–Fe(1)–C(4)	120.4(4)	C(3)–Fe(1)–C(4)	118.8(4)
Te(1)–Fe(2)–C(5)	178.9(4)	Te(1)–Fe(2)–C(6)	90.3(4)
C(5)–Fe(2)–C(6)	90.8(6)	Te(1)–Fe(2)–C(7)	89.4(4)
C(5)–Fe(2)–C(7)	90.1(5)	C(6)–Fe(2)–C(7)	118.5(5)
Te(1)–Fe(2)–C(8)	89.1(3)	C(5)–Fe(2)–C(8)	90.2(5)
C(6)–Fe(2)–C(8)	120.8(4)	C(7)–Fe(2)–C(8)	120.7(4)
Fe(1)–C(1)–O(1)	177.9(9)	Fe(1)–C(2)–O(2)	176.3(9)
Fe(1)–C(3)–O(3)	175.8(8)	Fe(1)–C(4)–O(4)	174.4(8)
Fe(2)–C(5)–O(5)	179.0(12)	Fe(2)–C(6)–O(6)	176.6(11)
Fe(2)–C(7)–O(7)	175.8(10)	Fe(2)–C(8)–O(8)	173.8(8)

<sup>a</sup> Symmetry operator: (a)  $-x, y, 0.5 - z$ .

an Au–Fe(2)–Fe(3) angle of 99.4(1)°. Each iron is bound to the capping telluride and three CO's as in the parent compound. All of the Fe–C–O angles are normal, averaging 175(2)°, as are the Fe–C and C–O bond distances, averaging 1.76(2) and 1.14(2) Å, respectively.

Metal clusters with edge-bridging  $[Au(PR_3)]^+$  groups are common, and since the early 1980's, cluster compounds containing one or more group IB metals have attracted a great deal of attention.<sup>22</sup> According to Evans and Mingos, when a  $(PR_3)Au$  group bridges a metal–metal bond, it can be viewed as a pseudoproton, using its  $a_1$  hybrid ( $s-z$ ) orbital to form a three-center, two-electron bond.<sup>23,24</sup>

**Structure and Bonding of  $[(C_6H_5)_4P]_2[\{Fe(CO)_4\}_4(\mu_4-Te)]$  (**III**).** The structure of **III** consists of a dianion with a central telluride bonded to four  $Fe(CO)_4$  fragments (Figure 3). The environment about the central telluride is tetrahedral, with Te–

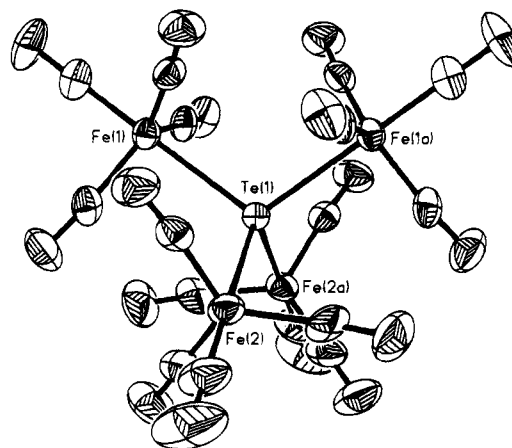


**Figure 3.** Thermal ellipsoid plot of  $[\{Fe(CO)_4\}_4Te]^{2-}$  (**III**). (Ellipsoids are at 35% probability.)

**Table 9.** Selected Bond Distances (Å) and Angles (deg) for **IV**

Distances			
I(1)–Fe(1)	2.666(1)	Te(1)–Te(2)	3.144(1)
Te(1)–Fe(1)	2.649(1)	Te(1)–Fe(2)	2.596(1)
Te(1)–Fe(3)	2.563(1)	Te(2)–Fe(1)	2.614(1)
Te(2)–Fe(2)	2.563(1)	Te(2)–Fe(3)	2.575(1)
Fe(1)–C(1)	1.775(7)	Fe(1)–C(2)	1.815(6)
Fe(1)–C(3)	1.817(7)	Fe(2)–Fe(3)	2.606(1)
Fe(2)–C(4)	1.778(10)	Fe(2)–C(5)	1.771(7)
Fe(2)–C(6)	1.789(9)	Fe(3)–C(7)	1.781(11)
Fe(3)–C(8)	1.782(7)	Fe(3)–C(9)	1.791(6)
O(1)–C(1)	1.148(10)	O(2)–C(2)	1.120(8)
O(3)–C(3)	1.127(8)	O(4)–C(4)	1.140(13)
O(5)–C(5)	1.145(9)	O(6)–C(6)	1.141(10)
O(7)–C(7)	1.146(14)	O(8)–C(8)	1.139(9)
O(9)–C(9)	1.141(8)		
Angles			
Te(2)–Te(1)–Fe(1)	52.8(1)	Te(2)–Te(1)–Fe(2)	52.0(1)
Fe(1)–Te(1)–Fe(2)	96.3(1)	Te(2)–Te(1)–Fe(3)	52.5(1)
Fe(1)–Te(1)–Fe(3)	96.7(1)	Fe(2)–Te(1)–Fe(3)	60.7(1)
Te(1)–Te(2)–Fe(1)	53.8(1)	Te(1)–Te(2)–Fe(2)	52.9(1)
Fe(1)–Te(2)–Fe(2)	98.0(1)	Te(1)–Te(2)–Fe(3)	52.1(1)
Fe(1)–Te(2)–Fe(3)	97.3(1)	Fe(2)–Te(2)–Fe(3)	61.0(1)
I(1)–Fe(1)–Te(1)	93.9(1)	I(1)–Fe(1)–Te(2)	166.9(1)
Te(1)–Fe(1)–Te(2)	73.4(1)	I(1)–Fe(1)–C(1)	95.5(3)
Te(1)–Fe(1)–C(1)	170.5(3)	Te(2)–Fe(1)–C(1)	97.3(3)
I(1)–Fe(1)–C(2)	87.8(3)	Te(1)–Fe(1)–C(2)	90.8(2)
Te(2)–Fe(1)–C(2)	89.2(3)	C(1)–Fe(1)–C(2)	90.2(3)
I(1)–Fe(1)–C(3)	87.9(3)	Te(1)–Fe(1)–C(3)	86.7(3)
Te(2)–Fe(1)–C(3)	94.4(3)	C(1)–Fe(1)–C(3)	93.0(3)
C(2)–Fe(1)–C(3)	174.9(3)	Te(1)–Fe(2)–Te(2)	75.1(1)
Te(1)–Fe(2)–Fe(3)	59.0(1)	Te(2)–Fe(2)–Fe(3)	59.8(1)
Te(1)–Fe(2)–C(4)	154.7(3)	Te(2)–Fe(2)–C(4)	92.1(2)
Fe(3)–Fe(2)–C(4)	95.6(3)	Te(1)–Fe(2)–C(5)	93.2(3)
Te(2)–Fe(2)–C(5)	160.9(2)	Fe(3)–Fe(2)–C(5)	101.3(2)
C(4)–Fe(2)–C(5)	92.6(4)	Te(1)–Fe(2)–C(6)	105.8(3)
Te(2)–Fe(2)–C(6)	100.2(2)	Fe(3)–Fe(2)–C(6)	156.3(3)
C(4)–Fe(2)–C(6)	97.8(4)	C(5)–Fe(2)–C(6)	97.5(3)
Te(1)–Fe(3)–Te(2)	75.4(1)	Te(1)–Fe(3)–Fe(2)	60.3(1)
Te(2)–Fe(3)–Fe(2)	59.3(1)	Te(1)–Fe(3)–C(7)	156.3(3)
Te(2)–Fe(3)–C(7)	91.4(3)	Fe(2)–Fe(3)–C(7)	96.1(3)
Te(1)–Fe(3)–C(8)	89.2(3)	Te(2)–Fe(3)–C(8)	157.3(2)
Fe(2)–Fe(3)–C(8)	98.7(2)	C(7)–Fe(3)–C(8)	96.8(4)
Te(1)–Fe(3)–C(9)	105.6(3)	Te(2)–Fe(3)–C(9)	103.0(3)
Fe(2)–Fe(3)–C(9)	158.5(3)	C(7)–Fe(3)–C(9)	96.4(4)
C(8)–Fe(3)–C(9)	97.1(3)	Fe(1)–C(1)–O(1)	179.1(8)
Fe(1)–C(2)–O(2)	176.0(7)	Fe(1)–C(3)–O(3)	176.3(9)
Fe(2)–C(4)–O(4)	176.7(8)	Fe(2)–C(5)–O(5)	176.7(7)
Fe(2)–C(6)–O(6)	174.9(9)	Fe(3)–C(7)–O(7)	179.0(7)
Fe(3)–C(8)–O(8)	178.2(8)	Fe(3)–C(9)–O(9)	174.8(8)

Fe–Te bond angles averaging 109.5° (see Table 8). An isoelectronic bismuth compound,  $[\{Fe(CO)_4\}_4(\mu_4-Bi)]^{3-}$ , has also been reported.<sup>25</sup> The Fe–Te bond lengths in **III** average

(22) Salter, I. D. *Adv. Organomet. Chem.* **1989**, *29*, 249.

(23) Mingos, D. M. P. *Polyhedron* **1984**, *3*, 1289.

(24) Evans, D. G.; Mingos, D. M. P. *J. Organomet. Chem.* **1982**, *232*, 171.

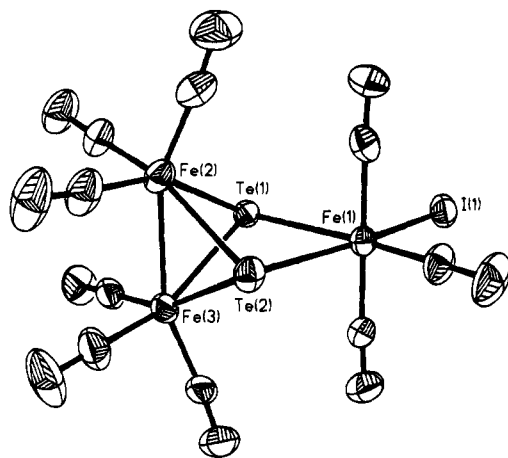


**Figure 4.** Thermal ellipsoid plot of [Fe<sub>3</sub>(CO)<sub>9</sub>Te]<sup>2-</sup> (IV). (Ellipsoids are at 35% probability.)

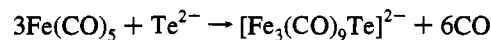
2.641(2) Å, which compare well with other reported Fe–Te bond lengths.<sup>7a,11c,12,26</sup> The Fe–C bonds average 1.77(2) Å, the C–O bonds 1.15(2) Å, and the Fe–C–O bond angles 176–(2)°, which are all comparable to values in other iron carbonyl main group clusters.

The bonding in the molecule is straightforward. If the central tellurium atom is considered to be in the 2– oxidation state, then all Fe(CO)<sub>4</sub> fragments are neutral. Each iron is ligated by four CO's and one pair of electrons from the central tellurium to complete its electron count. This type of coordination for heavy main group atoms has been observed before in molecules such as [Fe(CO)<sub>4</sub>]<sub>4</sub>(μ<sub>4</sub>-Q)]<sup>3-</sup> (Q = Sb, Bi),<sup>25</sup> [Co(CO)<sub>4</sub>]<sub>4</sub>(μ<sub>4</sub>-Bi)]<sup>-</sup>,<sup>27</sup> and [CoPPh<sub>3</sub>(CO)<sub>3</sub>]<sub>4</sub>Sb]<sup>+</sup>.<sup>28</sup>

**Structure and Bonding of [(C<sub>6</sub>H<sub>5</sub>)<sub>4</sub>P][Fe<sub>3</sub>Te<sub>2</sub>(CO)<sub>9</sub>I] (IV).** The structure of IV contains a dianion of the formula [Fe<sub>3</sub>Te<sub>2</sub>(CO)<sub>9</sub>I]<sup>2-</sup> with an isosceles triangle of iron atoms connected by two capping μ<sub>3</sub>-Te atoms and a single Fe–Fe bond of 2.606(1) Å (see Table 9). This bond is the hinge of an [Fe<sub>2</sub>Te<sub>2</sub>(CO)<sub>6</sub>]<sup>2-</sup> butterfly with each iron in the butterfly bonded to three CO's. Bonds from the hinge irons to each Te<sup>2-</sup> range from 2.563(1) to 2.596(1) Å and outline the wingtips of the butterfly. The tellurides are bridged by the unique iron, and these Fe–Te bonds are slightly longer, at 2.649(1) and 2.614–(1) Å. Three CO's and one I<sup>-</sup> complete the electron count around this bridging iron with an Fe–I distance of 2.666(1) Å. The I<sup>-</sup> lies trans to Te(2), and the geometry about Fe(1) is distorted octahedral with a Te(2)–Fe(1)–I(1) angle of 166.9–(1)° and a Te(1)–Fe(1)–I(1) angle of 93.9(1)°. The Te–Te distance is 3.144(1) Å, which is very similar to Te–Te distances in other compounds in this type and is normally considered to be outside the range of bonding interactions. The C–O distances are typical, averaging 1.14(1) Å, and the Fe–C–O angles average 177(2)°. The parent compound Fe<sub>3</sub>(CO)<sub>10</sub>Te<sub>2</sub> was first prepared in 1958,<sup>11</sup> and the phosphine derivative Fe<sub>3</sub>(μ<sub>3</sub>-Te)<sub>2</sub>(CO)<sub>9</sub>PPh<sub>3</sub> was structurally characterized in 1982.<sup>29</sup> The iodine derivative is isostructural and isoelectronic with both of these.

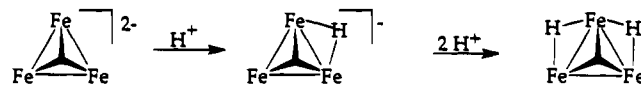
**Synthesis and Reactivity of [(C<sub>6</sub>H<sub>5</sub>)<sub>4</sub>P]<sub>2</sub>[Fe<sub>3</sub>(CO)<sub>9</sub>Te].** Reaction of a 3-fold excess of Fe(CO)<sub>5</sub> with a solution

containing a reduced telluride of nominal composition Te<sup>2-</sup> leads to the formation and isolation of I in excellent yield. Mild heat speeds up the reaction considerably. A possible balanced equation is



Infrared spectroscopy was used to monitor the reaction progress, and the IR spectrum of the product is quite distinctive in the carbonyl region. Since the spectrum of the reaction mixture is identical to that of the isolated product, and the product is isolated in excellent yield, it can be concluded that I is the dominant carbonyl-containing product in solution. It is not surprising that a cluster which contains only zerovalent iron centers is isolated from this reaction because the telluride source (Te<sup>2-</sup>) contains no Te–Te bonds which could oxidize the metal. It was previously reported that larger iron telluride clusters that contain iron atoms in the 1+ and 2+ oxidation states can be prepared by reacting Fe(CO)<sub>5</sub> with K<sub>2</sub>Te<sub>4</sub>, which contains Te–Te bonds to oxidize the metal center.<sup>7</sup> In addition, it has been reported that K<sub>2</sub>Te<sub>4</sub> will react with Fe(CO)<sub>3</sub>(η<sup>4</sup>-C<sub>4</sub>H<sub>6</sub>) in ethylenediamine in the presence of crypt to yield [Fe<sub>2</sub>(CO)<sub>6</sub>(μ-Te)(μ<sub>2</sub>,η<sup>1</sup>-Te<sub>2</sub>)]<sup>2-</sup>, which contains a unique (μ<sub>2</sub>,η<sup>1</sup>-Te<sub>2</sub>)<sup>2-</sup> ligand.<sup>9e</sup> Molecule I was also characterized by <sup>125</sup>Te NMR, and the shift of 361 ppm relative to (CH<sub>3</sub>)<sub>2</sub>Te falls well within the wide range of observed values for complexed tellurides.<sup>1b,30</sup> The ease and simplicity of the preparation of this compound make it an ideal candidate for reactivity studies.

**Reactions of [Fe<sub>3</sub>(CO)<sub>9</sub>(μ<sub>3</sub>-Te)]<sup>2-</sup> with Electrophiles.** Molecule I has been reacted with several hard and soft electrophiles, and in each case it can be concluded that the electrophile attacks an iron–iron bond. The reaction of I with the proton was investigated initially and monitored by <sup>1</sup>H NMR. The literature values of chemical shifts for a proton bound to a tellurium range from –8 to –13 ppm,<sup>31</sup> whereas those for protons bound to metal–metal bonds occur between –15 and –25 ppm.<sup>32</sup> Also, protons bound directly to a tellurium atom should display <sup>125</sup>Te satellites in their spectrum. Since the <sup>1</sup>H NMR of the reaction mixture containing 1 equiv of H<sup>+</sup> displays a peak at –22 ppm, while the mixture containing 2 equiv of H<sup>+</sup> shows a single peak near –24 ppm, we conclude that each H<sup>+</sup> attacked an iron–iron bond, generating three-center, two-electron bonds, and not a tellurium hydride. It should be noted that the metal-bridging hydride could be the thermodynamic product resulting from attack of the proton at the apical telluride followed by rearrangement. However, the low solubility of these salts prevents low-temperature NMR experiments which could resolve this point.



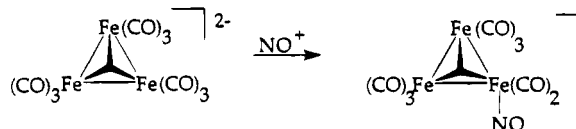
Since NO<sup>+</sup> is isoelectronic with CO and displays very strong π-back-bonding with transition metals, it was reacted with the title compound. It was anticipated that NO<sup>+</sup> could either substitute for one CO or act as a one-electron oxidant to form NO and oxidized clusters. Infrared spectroscopy was used to

- (25) (a) Churchill, M. R.; Fetting, J. C.; Whitmire, K. H.; Lagrone, C. B. *J. Organomet. Chem.* **1986**, *303*, 99. (b) Luo, S.; Whitmire, K. H. *Inorg. Chem.* **1989**, *28*, 1242.  
 (26) Bogan, L. E.; Rauchfuss, T. B.; Rheingold, A. L. *J. Am. Chem. Soc.* **1985**, *107*, 3843.  
 (27) Martinengo, S.; Fumagalli, A.; Ciani, G.; Moret, M. *J. Organomet. Chem.* **1988**, *347*, 413.  
 (28) Cobbleddick, R. E.; Einstein, F. W. B. *Acta Crystallogr.* **1979**, *B35*, 2041.  
 (29) Lesch, D. A.; Rauchfuss, T. B. *Organometallics* **1982**, *1*, 499.

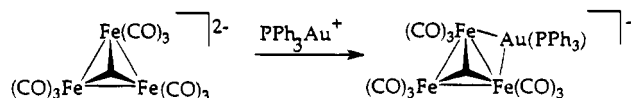
- (30) (a) Lesch, D. A.; Rauchfuss, T. B. *Inorg. Chem.* **1983**, *22*, 1854. (b) Herrmann, W. A.; Kneuper, H.-J. *J. Organomet. Chem.* **1988**, *348*, 193.  
 (31) (a) Herrmann, W. A.; Hecht, C.; Herdtweck, E.; Kneuper, H.-J. *Angew. Chem., Int. Ed. Engl.* **1987**, *26*, 132. (b) Hausmann, H.; Höfler, M.; Kruck, Th.; Zimmermann, H. W. *Chem. Ber.* **1981**, *114*, 975. (c) Küllmer, V.; Vahrenkamp, H. *Chem. Ber.* **1977**, *110*, 228. (d) DiVaira, M.; Peruzzini, M.; Stoppioni, P. *Inorg. Chem.* **1991**, *30*, 1001.  
 (32) Moore, D. S.; Robinson, S. D. *Chem. Soc. Rev.* **1983**, *12*, 415.



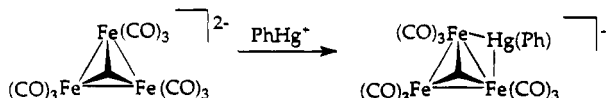
monitor these reactions. Complexes with terminal nitrosyl ligands exhibit very strong  $\nu(\text{NO})$  stretches in the range 1789–1664  $\text{cm}^{-1}$ , whereas doubly bridging nitrosyl ligands absorb in the range 1603–1445  $\text{cm}^{-1}$ .<sup>33</sup> Upon reaction of **I** with  $\text{NOBF}_4$ , gas evolution was observed and a very strong band appeared in the IR at 1713  $\text{cm}^{-1}$ . This stretch, which lies in the region for terminal nitrosyl ligands, leads us to believe the nitrosyl ligand has substituted for one CO ligand, generating  $[\text{Fe}_3(\text{CO})_8(\text{NO})\text{Te}]^-$ .



Since we hoped to observe reactivity at the apical telluride, we investigated the reactions of **I** with the much softer electrophiles  $(\text{PPh}_3)\text{AuCl}$  and  $\text{PhHgOAc}$ , and clean reactions were observed for both. A crystal structure was obtained for the product from the  $(\text{PPh}_3)\text{Au}^+$  reaction, **II**, and indicated that the electrophile again attacked at the iron–iron bond. Although



we were hoping that the  $(\text{PPh}_3)\text{Au}^+$  electrophile might bond with the soft tellurium instead of with the iron–iron bond, this result is not surprising. An isolobal analogy has been drawn between  $\text{H}^+$  and  $(\text{PPh}_3)\text{Au}^+$ ,<sup>23,24</sup> and in almost all compounds where structural comparisons are possible, the  $\text{Au}(\text{PR}_3)$  fragment occupies a position similar to that of the isolobal hydrido ligand in the related hydrido–metal cluster. In metal clusters containing a single coinage metal, the  $\text{M}(\text{PR}_3)$  group usually either bridges a metal–metal bond or caps a triangular three-metal face.<sup>22</sup> Several molecules such as  $[\text{AuRu}_3(\mu\text{-H})(\mu_3\text{-S})(\text{CO})_9(\text{PPh}_3)]$ <sup>34</sup> and  $[\text{AuCoFeRu}(\mu_3\text{-X})(\text{CO})_9(\text{PPh}_3)]$  ( $\text{X} = \text{S}, \text{PMe}$ )<sup>35</sup> were reported recently and have structures similar to **II**. When **I** was reacted with a second equivalent of  $(\text{PPh}_3)\text{AuCl}$ , a gold mirror formed on the bottom of the flask and the solution contained a suspended powder. Presumably, the reactant decomposed upon addition of a second  $(\text{PPh}_3)\text{Au}^+$  cation. Possibly, the starting product **I** is not a sufficiently large molecule to support two edge-bridging gold phosphine fragments. No crystal structure was obtained for the product of the reaction of **I** with  $\text{PhHg}^+$ ; however, the solution IR of the CO region of the product was obtained, and it is nearly superimposable with the solution IR of **II** (Figure 5). Therefore we can again conclude that the electrophile attacked at the metal–metal bond.



#### Reactions of $[\text{Fe}_3(\text{CO})_9(\mu_3\text{-Te})]$ with Oxidizing Agents.

When the reaction of  $\text{K}_2\text{Te}$  and excess iron pentacarbonyl was carried out in the presence of air,  $[\{\text{Fe}(\text{CO})_4\}_4(\mu_4\text{-Te})]^{2-}$ , **III**, was isolated in low (8%) yield. The product was analyzed by IR, elemental analysis, and X-ray crystallography. We do not

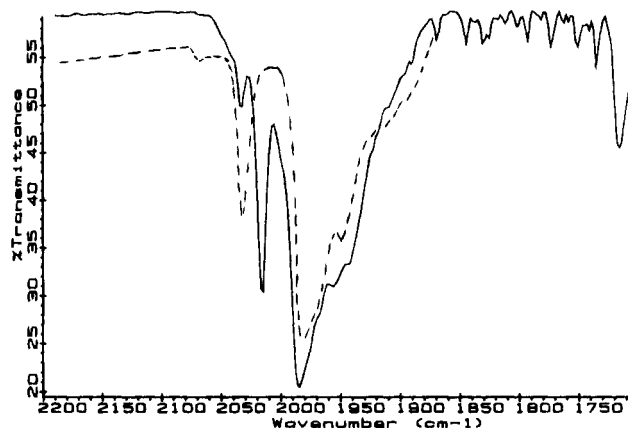
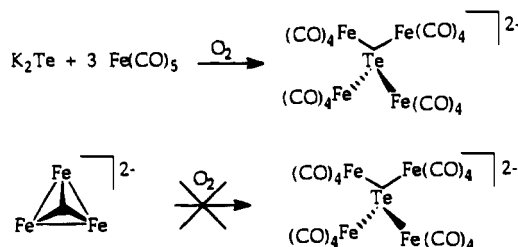


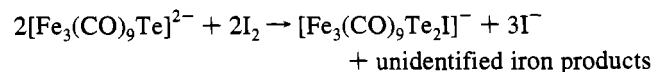
**Figure 5.** Overlapping IR spectra of  $\text{CH}_2\text{Cl}_2$  solutions of  $[(\text{PPh}_3)\text{AuFe}_3(\text{CO})_9\text{Te}]^-$  (**II**) and  $[(\text{PhHg})\text{Fe}_3(\text{CO})_9\text{Te}]^-$ . The solid spectrum represents **II**, and the dotted spectrum represents  $[(\text{PhHg})\text{Fe}_3(\text{CO})_9\text{Te}]^-$ .

think this product formed as a result of the oxidation of **I**. Instead, we believe that  $\text{K}_2\text{Te}$  reacts with excess  $\text{Fe}(\text{CO})_5$  in the presence of air to form **I**, and to form **III** also as a minor product. Since the former contains an open site on the tellurium atom, it can react quickly with air to decompose. However, the four  $\text{Fe}(\text{CO})_4$  fragments in the latter molecule provide steric protection from the oxygen, rendering it less reactive with air than the major product, **I**. With the decomposition of **I**, the minor product is left behind to crystallize. This accounts for the isolation of **III** in low yield. In support of this, only decomposition products are isolated if premade, crystalline  $[\text{Fe}_3(\text{CO})_9(\mu_3\text{-Te})]^{2-}$  is exposed to air, rather than the  $\text{Te}^{2-}/\text{Fe}(\text{CO})_5$  reaction mixture.



Reaction of **I** with  $\text{AgNO}_3$  provided inconclusive results. Since changes in color and the CO region of the IR occurred, we are certain reactions took place. Unfortunately, pure products could not be isolated, so the nature of the products could not be determined. No silver mirrors were observed, so simple oxidations resulting in neutral clusters probably did not occur. But shifts to higher wavenumbers in the CO region of the IR did occur, which is indicative of some type of oxidation or decrease of net charge throughout the cluster. It is possible that reactions with  $\text{AgNO}_3$  produced some type of oxidation, possibly leading to connection of cluster units by silver ions. Unfortunately, without single crystals this hypothesis could not be verified.

Molecule **I** reacted cleanly with  $\text{I}_2$ , shifting the CO region of the IR to higher wavenumbers, suggesting that a molecule with a less negative charge formed, either by addition of an  $\text{I}^+$  ion or by oxidation. Single crystals were isolated from the reaction of **I** with  $\text{I}_2$ , and analysis of **IV** showed that oxidation did occur along with addition of an iodide.



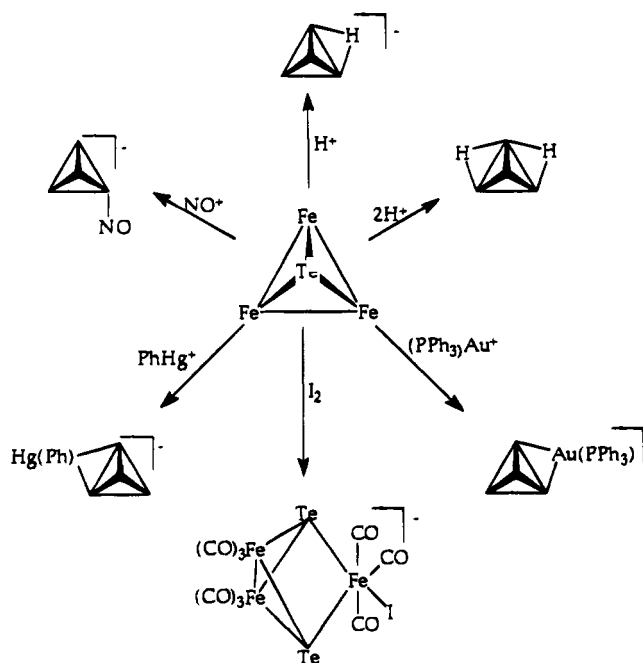
The product isolated is a derivative of the neutral  $\text{Fe}_3(\text{CO})_{10}$

(33) Gladfelter, W. L. *Adv. Organomet. Chem.* **1985**, *24*, 41.

(34) Bruce, M. I.; Shawkataly, O.; Nicholson, B. K. *J. Organomet. Chem.* **1985**, *286*, 427.

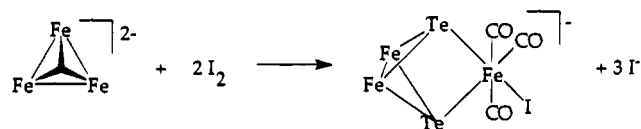
(35) Fischer, K.; Müller, M.; Vahrenkamp, H. *Angew. Chem., Int. Ed. Engl.* **1984**, *23*, 140.



**Scheme 1.** Summary Diagram of the Reactivity of [Fe<sub>3</sub>(CO)<sub>9</sub>Te]<sup>2-</sup>

Te<sub>2</sub> which has been known for several years.<sup>11,12c,26</sup> Several heterometallic derivatives of Fe<sub>3</sub>(CO)<sub>10</sub>Te<sub>2</sub> have been prepared by reacting either Fe<sub>3</sub>(CO)<sub>9</sub>Te<sub>2</sub> or Fe<sub>2</sub>(CO)<sub>6</sub>Te<sub>2</sub> with low-valent transition metal complexes such as [M(PPh<sub>3</sub>)<sub>2</sub>(C<sub>2</sub>H<sub>4</sub>)] (M = Pt, Pd) or [Co(CO)<sub>2</sub>(C<sub>5</sub>H<sub>5</sub>)].<sup>11e</sup> A majority of the resulting complexes contain an [Fe<sub>2</sub>(CO)<sub>6</sub>Te<sub>2</sub>]<sup>2-</sup> butterfly with the tellurium wingtips bridged by the heterometal. Although **IV** has a known molecular shape, its synthetic reaction is complicated, with three zerovalent iron tricarbonyl fragments undergoing formal oxidation to two Fe(I)'s and one Fe(II). Therefore instead of simple oxidation to produce a neutral species, or addition of I<sup>+</sup>, the

oxidation involves reaction of at least two molecules of **I** to produce a larger cluster. The nature of the inevitable iron-containing byproducts is not known.



### Summary and Conclusions

Excess Fe(CO)<sub>5</sub> reacts with a DMF solution of Te<sup>2-</sup> to form [Fe<sub>3</sub>(CO)<sub>9</sub>Te]<sup>2-</sup> in excellent yield. A variety of both hard and soft electrophiles react with **I**, and all apparently attack an iron-iron bond except for NO<sup>+</sup>, which replaces a CO (see Scheme 1). From these results we conclude that the lone pair on the tellurium is unreactive and the HOMO lies in the metal-metal bonds.

Reaction of **I** with AgNO<sub>3</sub> leads to inconclusive results. Since shifts to higher wavenumbers in the CO region of the IR did occur upon reaction, we are confident that the cluster was oxidized, but no products were characterized. Reaction with I<sub>2</sub> leads to formation of a larger cluster with substitution of an I<sup>-</sup>. Product **III** was isolated from the reaction of K<sub>2</sub>Te and excess Fe(CO)<sub>5</sub> with air. However **III** is probably not an oxidation product, but rather a byproduct that forms in low yield in the initial reaction mixture which is more resistant to oxidation than **I**.

**Acknowledgment.** We are indebted to the National Science Foundation for support of this research.

**Supplementary Material Available:** Complete listings of crystallographic data, atomic coordinates, bond distances and angles, anisotropic thermal parameters, and H atom coordinates for compounds **I-IV**, as well as a figure showing the disorder in compound **I** (31 pages). Ordering information is given on any current masthead page.

IC931177F